1 **Title**

2 Historical climate change and megafaunal extinctions linked to genetic diversity declines in
3 shorebirds.

4

5 **Author names and affiliations**

6 Hui Zhen Tan[1], Justin J.F.J. Jansen[2], Gary A. Allport[3], Kritika M. Garg[1,4], Balaji
7 Chattopadhyay[1,5], Martin Irestedt[6], Glen Chilton[7], Chyi Yin Gwee[1,8], and Frank E. Rheindt[1*]

8

9 [1]Department of Biological Sciences, National University of Singapore, 16 Science Drive 4,
10 Singapore 117558, Singapore

11 [2]Naturalis Biodiversity Center, Leiden, P.O. Box 9517, 2300 RA Leiden, The Netherlands

12 [3]BirdLife International, The David Attenborough Building, Pembroke Street, Cambridge, UK
13 CB2 3QZ

14 [4](Present address) Department of Biology, Ashoka University, Sonipat 131029, India

15 [5](Present address) Trivedi School of Biosciences, Ashoka University, Sonipat 131029, India

16 [6]Department of Bioinformatics and Genetics, Swedish Museum of Natural History, Stockholm,
17 Sweden

18 [7]Department of Biology, St. Mary's University, Calgary, Alberta, Canada.

19 [8](Present address) Division of Evolutionary Biology, Faculty of Biology, LMU Munich, Munich,
20 Germany

21

22 *Corresponding Author; e-mail: dbsrfe@nus.edu.sg

23

## Abstract

The impact of accelerated climate change on extinction risk is not well-characterised despite its increasing relevance. Comparative genomics of extinct versus extant species might be useful in elucidating broad trends in faunal endangerment. We investigated fluctuations in genetic diversity and extinction timing in our genomic dataset of nine species of particularly vulnerable migratory shorebirds (*Numenius*), including two species widely thought to be extinct. Most species faced generally sharp declines in effective population sizes, a proxy for genetic diversity, soon after the Last Glacial Maximum. During this time, a warming climate supported forest expansions at the expense of open habitats, exacerbated by human-induced mass extinctions of megafauna only a few thousand years prior, resulting in unprecedented reductions in shorebird breeding habitat. Species breeding in temperate regions, where they widely overlap with human populations, have been most strongly affected. Late Quaternary events can exert long-lasting effects on some species' susceptibility to extinction. Genomic inquiry is crucial in informing conservation actions in the fight against ongoing biodiversity loss.

## Introduction

Extinction is a natural and ongoing phenomenon, mostly occurring at low rates (Turvey & Crees, 2019). Occasionally, extreme events such as climate change lead to mass species extinctions and major biotic turnover (Crowley & North, 1988). Today, accelerating climate change is increasingly apparent, coinciding with elevated rates of species extinction that are 100–1000 times higher than the background rate (Koch & Barnosky, 2006; Pimm et al., 2014). While anthropogenic climate change is recognised as a major threat to biodiversity worldwide, the mechanisms by which it causes extinction, be it physiological stress, species interactions or other proximate causes, are not well characterised (Cahill et al., 2013). Investigations into the impact of anthropogenic climate change on species extinction risk are of paramount importance to inform conservation action in the fight against ongoing biodiversity loss (Frankham, 2005; Jetz et al., 2014; Urban, 2015).

The endangerment process and its associated conservation actions are usually viewed through a species-specific lens to pinpoint traits explaining a taxon's susceptibility to extinction. However, a universal approach based on genomic correlates of larger panels of species could add an important perspective to elucidate trends in faunal endangerment. Comparative genomics of extinct versus extant species are particularly useful in this context (Frankham, 2005), but have proven challenging in the past because of difficulties in obtaining viable genomic DNA from extinct taxa. Such comparisons can provide insights into past population trends to shed light on extinction risk in extant species.

We used a museomic approach to investigate fluctuations in genetic diversity in a genus of nine species of migratory shorebirds. Migratory shorebirds are threatened by warming temperatures and habitat loss in their breeding and wintering grounds respectively (Lemoine &

Böhning-Gaese, 2003). Curlews and whimbrels of the genus *Numenius*, which breed across the world's tundras and temperate grasslands, are particularly vulnerable to endangerment due to comparatively long generation times (Pearce-Higgins et al., 2017). Our study includes two species, the slender-billed curlew (*N. tenuirostris*) and Eskimo curlew (*N. borealis*), that are presumably extinct (Buchanan et al., 2018; Butchart et al., 2018; Kirwan, Porter, & Scott, 2015; Pearce-Higgins et al., 2017; Roberts, Elphick, & Reed, 2010; Roberts & Jarić, 2016). We acquired 67 ancient and fresh samples from all nine *Numenius* species and most known subspecies (Figure 1A; Table S1) for target enrichment. After filtering, a final alignment of 514,771bp across 524 sequence loci were retained for each of 62 samples at a mean coverage of 118X.

## Results and discussion

Phylogenomic analyses using MP-EST (L. Liu, Yu, & Edwards, 2010) revealed two separate groups, here called the "whimbrel clade" and the "curlew clade", that diverged approximately 5 million years ago (Figure 1B; Figure S1A). This is the first phylogenomic analysis consisting of all members of the genus *Numenius*. The use of degraded DNA from toepads of museum specimens allowed us to include the two presumably extinct taxa. Of these, the slender-billed curlew emerged as sister to the Eurasian curlew (*N. arquata*), a phenotypically similar species with which it overlapped in its Central Asian breeding range (Sharko et al., 2019). On the other hand, the Eskimo curlew emerged as a distinct member of the curlew clade with no close relatives (Figure 1B). Our phylogenomic dating analyses demonstrated that 40.6% of the evolutionary distinctness (Jetz et al., 2014) of the curlew clade has been lost with the presumable extinction of the two species, and another 15% is endangered (Figure 1B; Table S2), rendering this one of the most extinction-prone bird groups globally.

To further characterise the differential impact of extinction pressures, we characterised the demographic history of each species and considered them in the context of key climatic and biotic events. Reconstruction of fluctuations in effective population size ($N_e$), a proxy for genetic diversity, using stairway plot (X. Liu & Fu, 2015) revealed generally sharp declines in most species that accelerated ~11,000 years ago (kya) and continued to the present day for some species (Figure 1C). Preceding the onset of this decline (50–10kya), cooling events leading up to the LGM allowed tundra habitats to dominate and saw great increases in $N_e$ in the tundra-inhabiting Eurasian whimbrel (*N. phaeopus*) (Binney et al., 2017; Zimov et al., 1995). At the same time, widespread megafaunal extinction was underway due to both climate change and the arrival of early *Homo sapiens* that carried out hunts (Figure 1C) (Koch & Barnosky, 2006). Without functional replacements for the ecosystem-engineering effects of grazing megafauna, temperate grasslands and steppes were not maintained (Bakker et al., 2016). With the end of the last glacial period and the onset of a warming interglacial climate, forests expanded at the expense of open habitats (Binney et al., 2017). This displacement lowered the carrying capacity for megafauna and led to further population declines, forming a feedback loop (Koch & Barnosky, 2006). Therefore, post-glacial warming and megafaunal extinction may have acted synergistically in producing unprecedented reductions of open landscapes for breeding and concomitant sharp declines in the genetic diversity of *Numenius* shorebirds.

In the late Holocene, climate regimes have been relatively stable compared to that of the last glacial period (Dansgaard et al., 1993). However, members of the curlew clade, which predominantly breed in temperate grasslands and steppes, persistently exhibit levels of $N_e$ that are an order of magnitude lower than those of the tundra-inhabiting whimbrels (Figure 1C). After declines in $N_e$ in the post-glacial Holocene, whimbrels seem to have stabilised in genetic

diversity starting at ~700 years ago while curlews have continued to decline. The fates of these two *Numenius* clades appear to have diverged at the onset of post-glacial warming. Whimbrels accumulated and maintained genetic diversity during glacial periods when ice-free tundra habitats in Far Eastern Siberia and Alaska were expansive (Bigelow et al., 2003; Binney et al., 2017). In contrast, curlews were forced into smaller temperate glacial refuges and would have suffered great reductions in genetic diversity, incurring extinction debt (Kuussaari et al., 2009; Tan et al., 2019; Urban, 2015). Presently, temperate grasslands, where curlews breed, face far greater anthropogenic pressures through various land use regimes than the northerly tundra (Pimm et al., 2014), contributing to continued declines of curlews more so than whimbrels. In particular, genetic diversity was lowest in the presumably extinct slender-billed curlew, *N. tenuirostris* (Figure 1C). A low genetic diversity decreases the evolutionary potential for adaptations to environmental change and increases susceptibility to inbreeding depression, raising a species' extinction risk (Frankham, 2005).

The plight of these curlews may be mirrored by other species as the world's biodiversity becomes increasingly threatened, with unknown consequences for ecosystems (Pimm et al., 2014). Our work emphasises that genomic inquiries into past genetic diversity trends can inform present-day conservation action by revealing bottleneck events and pinpointing populations with a depauperate genetic diversity. We also highlight the unique challenges faced by grassland biomes and biota that warrant more conservation attention (Török, Ambarlı, Kamp, Wesche, & Dengler, 2016).

Our study revealed that climatic and environmental changes impacted the genetic diversity of curlews, with similar declines documented in other grassland-dependent biota (Ceballos et al., 2010; Chan, Lacey, Pearson, & Hadly, 2005; Helm et al., 2009; Nakahama, Uchida, Ushimaru,

& Isagi, 2018; Wesche et al., 2016). Late Quaternary climate change and megafaunal extinction may have had cascading effects onto species' endangerment that have lasted to the present day. This work provides a glimpse into how biodiversity may – in the future – respond to unabating anthropogenic climate change.

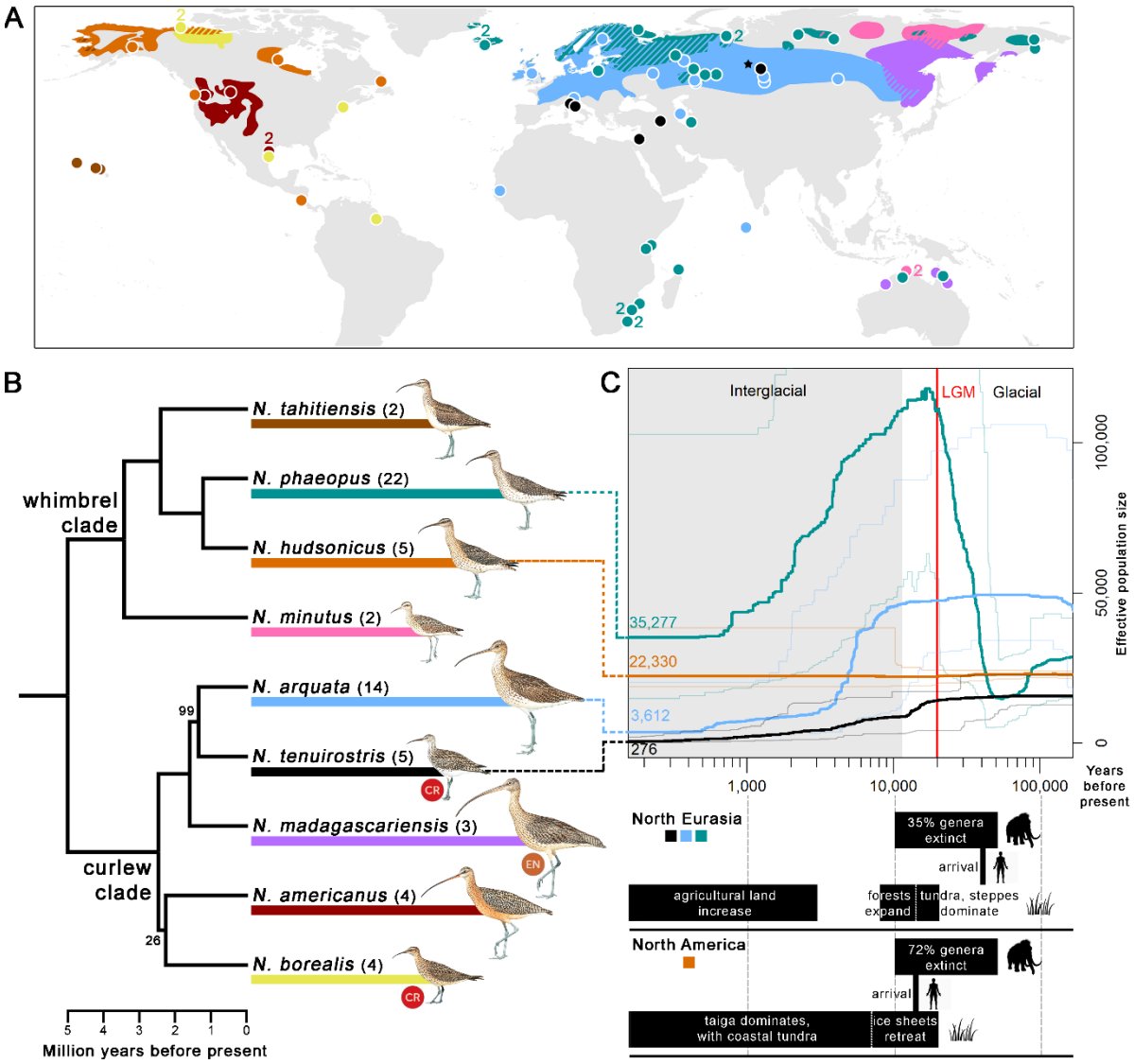


Figure 1. (A) Breeding distribution map and sampling localities of all *Numenius* species. Colours correspond to species identities in the tree in (B). Diagonal lines denote regions with co-distributed species. Each circle represents one sample unless otherwise specified by an adjacent number. The only known breeding records of *N. tenuirostris* were from near the village of Krasnoperova c.10 km south of Tara, Omsk (Russia), which is denoted with a black star (★), although this might not have been the core breeding area. (B) Phylogenomic tree constructed from an alignment of 514,771bp across 524 sequence loci. Tree topology (including bootstrap support values) and

142 divergence times were estimated with MP-EST and MCMCTree respectively. Only bootstrap <100 is displayed.
143 Sample sizes for each species are given in brackets. IUCN Red List status of critically endangered (CR) and
144 endangered (EN) species are indicated. Illustrations of *Numenius* birds were reproduced with permission from Lynx
145 Edicions. (C) Demographic history reconstruction using stairway plot for all species represented by ≥5 samples,
146 which is the minimum number of samples required. Line colours correspond to species identities in the tree in (B)
147 and numbers at present time represent the present-day effective population size. Thick lines represent the median
148 effective population size while thin lines represent the 2.5 and 97.5 percentile estimation respectively. The grey-
149 shaded panel indicates the current interglacial period and the red line denotes the Last Glacial Maximum (LGM).
150 Black bars below the plot provide key dates of megafaunal extinction events(Koch & Barnosky, 2006), *Homo*
151 *sapiens* arrival(Koch & Barnosky, 2006) and climatic change for northern Eurasia(Binney et al., 2017) and North
152 America(Bigelow et al., 2003) respectively. The timing of these events is indicated with light grey dashed lines
153 extending downwards from the time axis.

154

155 **Materials and methods**

156 Taxon sampling

157 We acquired samples for all nine species in the genus *Numenius*, encompassing most of
158 the known subspecies. Species and subspecies identities are as provided by the source museum
159 or institution (Table S1) or assigned in reference to known breeding and wintering locations
160 (Billerman, Keeney, Rodewald, & Schulenberg, 2020). We also included one common redshank
161 *Tringa totanus* as an outgroup for phylogenetic rooting. Most samples were acquired through
162 museum loans except for an individual of the endangered subspecies *N. phaeopus alboaxillaris*
163 that was sampled during fieldwork by GA (Table S1). Where possible, we acquired fresh
164 samples (tissue or blood) for their higher quality of genetic information. To represent rarely
165 sampled or presently rare taxa for which no fresh samples were available, we acquired toepad
166 material from historic museum specimens and applied ancient DNA methods.

167 Baits design for target capture

168 We used the *Calidris pugnax* genome (GCA_001458055.1) (Küpper et al., 2015) to
169 design baits to capture selected exons. We used EvolMarkers (C. Li, Riethoven, & Naylor, 2012)
170 to identify single-copy exons conserved between *C. pugnax, Taeniopygia guttata* (accession no.

GCF_003957565.1; released by the Vertebrate Genomes Project) and *Ficedula albicollis* (accession no. GCA_000247815.1). Exons longer than 500bp with a minimum identity of 55% and an e-value $< 10e^{-15}$ were isolated with bedtools 2.28.0 (Quinlan & Hall, 2010), forming our target loci. Only target loci with 40–60% GC content were retained and any overlapping loci were merged (Quinlan & Hall, 2010). Finally, target loci with repeat elements were filtered out in RepeatMasker 4.0.6 (Smit, Hubley, & Green, 2015). We arrived at a final set of 565 unique target loci with a mean length of 970bp. These target loci were used to design 19,003 100bp-long biotinylated RNA baits at 4X tiling density (MYcoarray/Arbor Biosciences, USA).

Laboratory methods

Both fresh and ancient samples were subjected to DNA extraction, followed by library preparation and target enrichment, with slight modifications for various sample types to optimise yield. DNA extractions of fresh samples were performed using the DNEasy Blood & Tissue Kit (Qiagen, Germany) with an additional incubation step with heat-treated RNase. Extractions for ancient samples were performed using the same kit but with modifications to reagent volumes and extraction columns (Chattopadhyay, Garg, Mendenhall, & Rheindt, 2019). Ancient samples were processed in a dedicated facility for highly degraded specimens.

DNA extracted from fresh samples was sheared via sonification using Bioruptor Pico (Diagenode, Belgium) to a target size of 250bp. DNA extracts from ancient samples were generally smaller than the target size; hence no further shearing was performed. Whole-genome libraries were prepared using the NEBNext Ultra™ II DNA Library Prep Kit for Illumina (New England Biolabs, Ipswich, USA) with modifications for subsequent target enrichment. For fresh samples, adaptor concentrations were kept constant regardless of DNA input amount. Size selection with AMPure XP beads (Beckman Coulter, USA) was performed for 250bp insert

sizes. The reaction was split into two equal parts before polymerase chain reaction (PCR) amplification and combined afterwards for subsequent steps. For ancient samples, a formalin-fixed, paraffin-embedded (FFPE) DNA repair step was first performed using NEBNext FFPE DNA Repair Mix (New England BioLabs). A 10-fold dilution of adaptors was used, and no size selection was performed. For both types of samples, twelve cycles of PCR amplification were performed.

Target enrichment was carried out using the MYbaits manual (Arbor Biosciences, USA) with modifications (Chattopadhyay et al., 2019). We used 1.1uL of baits per fresh sample (~5X dilution) and 2.46 uL of baits per ancient sample (~2X dilution). For fresh samples, hybridization of baits and target loci was performed at 65°C for 20 hours and 15 cycles of amplification were performed. For ancient samples, hybridization was performed at 60°C for 40 hours, and 20 cycles of amplification were performed. For both fresh and ancient samples, one negative control sample was added for each batch of extraction, library preparation and target enrichment. Extracts, whole-genome libraries, final enriched libraries, and all negatives were checked for DNA concentration on a Qubit 2.0 Fluorometer using the Qubit dsDNA HS assay kit (ThermoFisher Scientific, USA), and were checked for fragment size on a Fragment Analyzer using the HS NGS Fragment kit (1–6000bp) (Agilent Technologies Inc., USA). Final enriched libraries were pooled at equimolar quantities. A total of 67 enriched libraries were sequenced, with fresh and ancient samples sequenced separately on two Illumina HiSeq 150bp paired-end lanes (NovogeneAIT, Singapore).

Reference genome assembly

We obtained a sample of *N. phaeopus* (ZMUC 112728) from Natural History Museum of Denmark, Copenhagen and genomic DNA was extracted using the KingFisher™ Duo Prime

Magnetic Particle Processor (ThermoFisher Scientific, USA) and the KingFisher Cell and Tissue DNA Kit (Thermo Fisher Scientific). A linked-read sequencing library was prepared using the Chromium Genome library kits (10X Genomics) and sequenced on one Illumina Hiseq X lane at SciLifeLab Stockholm (Sweden). The *de novo* assembly analysis was performed using 10X Chromium Supernova (v. 2.1.1). Reads were filtered for low quality and duplication and assemblies were checked for accuracy and coverage and the best assembly was selected based on higher genome coverage with fewer errors. The final genome had a size of 1.12Gb at a coverage of 50X with N50 = 3504.2kbp.

Raw reads processing

Raw reads were checked for sequencing quality in FastQC 0.11.8 (Babraham Bioinformatics). Reads were trimmed for low-quality termini and adaptors in fastp 0.20.0 (Chen, Zhou, Chen, & Gu, 2018). We retained reads with a minimum length of 36bp and set a phred quality threshold of 20. Retained reads started at the first base satisfying minimum quality criteria at the 5'-end and were truncated wherever the average quality fell below the threshold in a sliding window of 5bp. Duplicates were also removed using FastUniq 1.1 (Xu et al., 2012) before sequence quality, duplication rate and adaptor content were checked again in FastQC. We employed FastQ Screen 0.14.0 (Wingett & Andrews, 2018) to assign the source of DNA against a list of potential contaminants. We aligned reads to the assembled *Numenius phaeopus* genome, *Homo sapiens* (accession no. GCF_000001405.39) and a concatenated database of all available bacterial genomes available on GenBank("National Center for Biotechnology Information (NCBI)," 1988). Only reads that mapped uniquely to the *N. phaeopus* genome were retained. Reads were sorted and re-paired using BBtools 37.96 (Bushnell, 2014). Downstream

bioinformatic procedures were split into single nucleotide polymorphism (SNP)-based and sequence-based analyses.

SNP calling

For SNP-based analyses, reads were aligned to the target sequences used for bait design using bwa-mem 0.7.17 (Li, 2013). The output alignment files were converted to bam files (view) and sorted by coordinates (sort) using SAMtools 1.9 (Li et al., 2009). Alignments were processed in Picard 2.20.0 (Picard tools, Broad Institute, Massachusetts, USA) to add read group information (AddOrReplaceReadGroups), and another round of duplicate identification was performed (MarkDuplicates) before alignment files were indexed (BuildBamIndex). The reference file of target sequences was indexed in SAMtools (faidx) and a sequence dictionary was created in Picard (CreateSequenceDictionary). To improve SNP calling accuracy, indel realignment was performed in GATK 3.8 (McKenna et al., 2010) (RealignerTargetCreator, IndelRealigner). We inspected ancient DNA alignments in mapDamage 2.0.9 (Jónsson, Ginolhac, Schubert, Johnson, & Orlando, 2013) and trimmed up to 5bp from the 3' ends of both reads to minimise frequencies of G to A misincorporation (<0.1) and soft clipping (<0.2). Finally, alignments were checked for quality and coverage in QualiMap 2.2.1 (Okonechnikov, Conesa, & García-Alcalde, 2016).

We first generated likelihoods for alignment files in BCFtools 1.9 (Li, 2011) (mpileup), skipping indels. Using the same program, we then called SNPs (call) using the multiallelic and rare-variant calling model. Called SNPs were filtered in VCFtools 0.1.16 (Danecek et al., 2011) to retain sites with quality values >30, mean depth 30–150, minor allele frequency ≥0.02 and missing data <5%, in the listed order. Missingness and depth in sites and individuals, respectively, were quantified for SNPs called. We remove eight individuals from downstream

analyses due to a combination of missing data (>0.4%) and low coverage (<36X). A Perl script was used to call one SNP per locus to avoid calling linked SNPs. SNPs were further screened for linkage disequilibrium in PLINK 1.9 (Purcell et al., 2007) using a sliding window of 50 SNPs with a step size of 10 and an $r^2$ correlation threshold of 0.9. Finally, we also screened for neutrality of SNPs in BayeScan 2.1 (Foll & Gaggiotti, 2008) using default settings. We created dedicated SNP sets for input into demographic history reconstruction methods by applying the method as described above but without minor allele frequency cut-offs and with all SNPs in each locus retained.

Population genomic analyses

We conducted principal component analysis (PCA) for all *Numenius* samples using SNPRelate 1.16.0 (Zheng et al., 2012) in R 3.5.1 (R Core Team, 2018) (Figure S1A). We did not detect any considerable genomic differentiation along subspecific lines within *N. phaeopus* and *N. arquata*, whose population-genetic structure had been resolved with thousands of genome-wide markers in a previous study (Tan et al., 2019) (Figure S1B, C). Samples of *N. p. alboaxillaris* and *N. a. suschkini*, two Central Asian taxa that are described in literature as phenotypically differentiated (Allport, 2017; Engelmoer & Roselaar, 1998b, 1998a; Morozov, 2000), did not emerge as genomically distinct from other conspecific populations and are likely to represent ecomorphological adaptations controlled by few genes. Sample NBME 1039630, which was identified as *N. tenuirostris*, and sample MCZR 15733, which was identified as an *N. arquata* that shares many morphological features with *N. tenuirostris*, clustered with *N. arquata* samples (Table S1, Figure S1D). Both samples were assigned as *N. arquata* in subsequent phylogenetic analyses.

Sequence assembly

For sequence-based analyses, reads were assembled using HybPiper 1.3.1 (Johnson et al., 2016) (reads_first) to yield sequence loci. Firstly, reads were mapped to the target sequences using BWA 0.7.17 (Li & Durbin, 2009) and sorted by gene. Contigs were then assembled from the reads mapped to respective loci using SPAdes 3.13 (Bankevich et al., 2012) with a coverage cutoff value of 20. Using Exonerate 2.4.0 (Slater & Birney, 2005), these contigs were then aligned to the target sequences and sorted before one contig per locus was chosen to yield the final sequences. We inspected locus lengths (get_seq_lengths) and recovery efficiency (hybpiper_stats) across all loci. We then investigated potentially paralogous loci (paralog_investigator) by building gene trees using FastTree 2.1.11 (Price, Dehal, & Arkin, 2010) (paralog_retriever), and 10 identified loci were removed. All loci retained were present in at least 80% of individuals and constituted at least 60% of the total target loci length. In summary, a total of 525 loci were recovered from 62 samples.

Phylogenomic analyses

Multisequence alignment was performed for each locus using MAFFT 7.470 (Katoh & Standley, 2013), allowing for reverse complement sequences as necessary. Alignments were checked for gaps using a custom script, and loci with >35% gaps were removed from downstream analyses. A total alignment length of 514,771bp was obtained.

Phylogenomic analyses were performed on a concatenated dataset as well as on individual gene trees. Concatenation was performed with abioscript 0.9.4 (Larsson, 2010) (seqConCat). For the concatenated dataset, we constructed maximum-likelihood (ML) trees using RAxML 8.2.12 (Stamatakis, 2014) with 100 alternative runs on distinct starting trees. We applied the general time reversible substitution model with gamma distributed rate variation

among sites and with estimation of proportion of invariable sites (GTR+I+G) (Abadi, Azouri, Pupko, & Mayrose, 2019; Arenas, 2015).

For individual gene trees, the best substitution model for each locus was determined using jModelTest 2.1.10 (Darriba, Taboada, Doallo, & Posada, 2012) by virtue of the corrected Akaike information criterion value. We then constructed ML trees in PhyML 3.1 with the subtree pruning and regrafting algorithm, using 20 initial random trees. We performed 100 bootstrap replicates with ML estimates for both proportion of invariable sites and value of the gamma shape parameter. Individual gene trees were then rooted with Newick Utilities 1.3.0 (Junier & Zdobnov, 2010). We removed one locus from downstream analyses due to the absence of outgroup sequence such that 524 loci were retained across 62 samples.

Species tree analyses were performed using the rooted trees in MP-EST 1.6 (L. Liu et al., 2010), without calculation of triple distance among trees. We grouped samples by species and performed three runs of 10 independent tree searches per dataset (Cloutier et al., 2019). To calculate bootstrap values of the species tree, we performed multi-locus, site-only resampling (Mirarab, 2014) from the bootstrap trees (100 per gene) output from PhyML. The resulting 100 files, each with 100 bootstrap trees, were rooted and species tree analyses were performed in the same manner for each file in MP-EST. The best tree from each run was identified by the best ML score and compiled. Finally, we used the majority rule in PHYLIP 3.695(Felsenstein, 2009) to count the number of times a group descending from each node occurred so as to derive the bootstrap value (consense).

For estimation of divergence times, we applied MCMCtree and BASEML 4.9e (Reis & Yang, 2011), a package in PAML (Yang, 2007). To prepare the molecular data from 62 samples and 524 loci, we compiled the DNA sequence of each sample and combined all samples onto

separate rows of the same file. We then obtained consensus sequences for each species using Geneious Prime 2020.2 (Kearse et al., 2012), with a majority support threshold of 50% and ignoring gaps. We visually checked the resulting consensus sequences to ensure that ambiguous bases remained infrequent. Consensus sequences were organised by loci as per the input format for MCMCtree. We then prepared the input phylogenetic tree using the topology estimated in MP-EST with fossil calibrations of the two most basal nodes, namely between our outgroup (*Tringa totanus*) and all *Numenius* species, as well as that between the whimbrel and curlew clades within *Numenius*. Due to a lack of known fossils within the genus *Numenius*, we performed further calibrations using p-distance values calculated from the COI sequences of *Numenius* species. We applied the bird COI mutation rate of 1.8% per million year (Lavinia, Kerr, Tubaro, Hebert, & Lijtmaer, 2016) and converted mean, maximum and minimum p-distance values of both nodes to time (100 million years ago (MYA)). We maintained a conservative position and scaled the COI-based timings by a factor of two to obtain the final lower and upper bounds of node timings. We used the default probability of 0.025 that the true node age is outside the calibration provided.

To run MCMCtree, we first calculated the gradient and Hessian matrix of the branch lengths with the GTR substitution model applied and using default values of gamma rates and numbers of categories (mcmctree-outBV.ctl). We then performed two independent Markov chain Monte Carlo (MCMC) samplings of the posterior distribution of divergence times and rates (mcmctree.ctl). All default values were used except that a constraint on the root age was set to <0.3 (100 MYA). We also varied the prior for the birth-death process with species sampling and ensured that time estimates are not affected by the priors applied (dos Reis & Yang, 2019). We then performed convergence diagnostics for both runs using R to ensure that posterior means are

similar among multiple runs, ensuring that the parameter space has been explored thoroughly by the MCMC chain. Finally, we conducted MCMC sampling from the prior with no data to check the validity of priors used by comparing them with posterior times estimated. Again, two independent MCMC samplings were performed with convergence diagnostics.

Phylogenetic trees were visualised in FigTree 1.4.4 (Rambaut, 2018) with bootstrap values and node ages (MYA) including the 95% credibility intervals. Evolutionary distinctness and phylogenetic diversity was calculated for each branch (Jetz et al., 2014) using the divergence times estimated in MCMCTree.

Demographic history reconstruction

We derived trends in effective population size using stairway plot 2.1.1 (X. Liu & Fu, 2015) applying the recommended parameters. From the dedicated SNP sets that were created without minor allele frequency cut-off, we calculated a folded site frequency spectrum using vcf2sfs.py 1.1 (Marques, Lucek, Sousa, Excoffier, & Seehausen, 2019). We ran stairway plots for each species with five or more samples, as recommended for accurate inference (stairway_plot_es Stairbuilder). We assumed a mutation rate per site per generation of $8.11e^{-8}$, as estimated for shorebirds in the same order as *Numenius* (Charadriiformes) (Wang et al., 2019), and respective generation times of 5–8 years respectively (Bird et al., 2020; IUCN, 2020).

**Acknowledgements**

We thank the following personnel and institutions for the generous contribution of samples (Table S1): Paul Sweet and Thomas Trombone at the American Museum of Natural History (AMNH, New York); Robert Palmer and Leo Joseph at the Australian National Wildlife Collection (ANWC, Canberra); Molly Hagemann at the Bernice Pauahi Bishop Museum

(BPBM, Hawaii); David Allan at the Durban Natural Science Museum (DNSM, Durban) and Celine Santillan who assisted in sample transport; Ben Marks at the Field Museum of Natural History (FMNH, Chicago); Foo Maosheng at the Lee Kong Chian Natural History Museum (LKCNHM, Singapore); Carla Marangoni and Gloria Svampa at the Museo Civico di Zoologia (MCZR, Rome); Henry McGhie at the University of Manchester, Manchester Museum (MMUM, Manchester); Robert Prŷs-Jones, Mark Adams, Alex Bond, Ari Benucci and Douglas Russell at the Natural History Museum, London (NHMUK, Tring); Manuel Schweizer at the Naturhistorisches Museum der Bürgergemeinde Bern (NMBE, Bern); Bob McGowan at the Natural Museum of Scotland (NMS, Edinburgh); Joanna Sumner at Museums Victoria (NMV, Melbourne); Angela Ross at the National Museums NI (NMNI, Northern Ireland) and David Allen and Graeme Buchanan who assisted in sample transport; Jan Bolding Kristensen at the Natural History Museum of Denmark (SNM, Copenhagen); José Alves and Camilo Carneiro at the University of Iceland (UOI, Reykjavik); Sharon Birks at the Burke Museum, University of Washington (UWBM, Washington); Pavel S. Tomkovich, Dmitry Shitikov and Vladimir Sotnikov at the Zoological Museum of Moscow State University (ZMMU, Moscow); and Fyodor Kondrashov and Lisa Chilton who assisted in sample transport. Fletcher Smith assisted in Mozambique (with permission from Lucilia Chuquela, Museu de História Natural and Universidade Eduardo Mondlane, Maputo) with further assistance from Rebecca and Cyril Kormos, Patricia Zurita and Vinayagan Dhamarajah. HZT acknowledges Elize Ying Xin Ng, Pratibha Baveja, Yong Chee Keita Sin, Shivaram Rasu, Dominic Yong Jie Ng, and Wu Meng Yue for assistance in laboratory procedures and analyses. The authors acknowledge support from the National Genomics Infrastructure in Stockholm funded by Science for Life Laboratory, the Knut and Alice Wallenberg Foundation and the Swedish Research Council, and SNIC/Uppsala

Multidisciplinary Center for Advanced Computational Science for assistance with massively parallel sequencing and access to the UPPMAX computational infrastructure. KMG acknowledges support from the DBT-Ramalingaswami Fellowship (No. BT/HRD/35/02/2006). BC acknowledges funding from the South East Asian Biodiversity Genomics (SEABIG) Grant (numbers WBS R-154-000-648-646 and WBS R-154-000-648-733) and startup funding from Trivedi School of Biosciences, Ashoka University.

## Competing interests

The authors declare no competing interests.

## Author Contributions

FER, JJFJJ, GAA, HZT conceptualised the research aims. JJFJJ, GAA, GC and HZT collected samples, KMG and BC designed the probes set and MI constructed the reference genome. HZT performed all laboratory procedures with guidance from CYG, KMG and BC. HZT performed all bioinformatic analyses with guidance from CYG and FER. HZT and FER produced the initial draft of the manuscript which was reviewed by all co-authors.

## References

Abadi, S., Azouri, D., Pupko, T., & Mayrose, I. (2019). Model selection may not be a mandatory step for phylogeny reconstruction. *Nature Communications*, *10*(1), 1–11. https://doi.org/10.1038/s41467-019-08822-w

Allport, G. (2017). Steppe Whimbrels *Numenius phaeopus alboaxillaris* at Maputo, Mozambique, in February–March 2016, with a review of the status of the taxon. *Bulletin of the African Bird Club*, *24*(1), 1–12.

Arenas, M. (2015). Trends in substitution models of molecular evolution. *Frontiers in Genetics*, *6*(OCT), 319. https://doi.org/10.3389/fgene.2015.00319

Bakker, E. S., Gill, J. L., Johnson, C. N., Vera, F. W. M., Sandom, C. J., Asner, G. P., & Svenning, J. C. (2016). Combining paleo-data and modern exclosure experiments to assess the impact of megafauna extinctions on woody vegetation. *Proceedings of the National Academy of Sciences of the United States of America*, *113*(4), 847–855. https://doi.org/10.1073/pnas.1502545112

426 Bankevich, A., Nurk, S., Antipov, D., Gurevich, A. A., Dvorkin, M., Kulikov, A. S., … Pevzner,
427 P. A. (2012). SPAdes: A new genome assembly algorithm and its applications to single-cell
428 sequencing. *Journal of Computational Biology*, *19*(5), 455–477.
429 https://doi.org/10.1089/cmb.2012.0021

430 Bigelow, N. H., Brubaker, L. B., Edwards, M. E., Harrison, S. P., Prentice, I. C., Anderson, P.
431 M., … Volkova, V. S. (2003). Climate change and Arctic ecosystems: 1. Vegetation
432 changes north of 55°N between the last glacial maximum, mid-Holocene, and present.
433 *Journal of Geophysical Research: Atmospheres*, *108*(19), 8170.
434 https://doi.org/10.1029/2002jd002558

435 Billerman, S. M., Keeney, B. K., Rodewald, P. G., & Schulenberg, T. S. (Eds.). (2020). *Birds of*
436 *the World*. Ithaca, NY, USA: Cornell Laboratory of Ornithology. Retrieved from
437 https://birdsoftheworld.org/bow/home

438 Binney, H., Edwards, M., Macias-Fauria, M., Lozhkin, A., Anderson, P., Kaplan, J. O., …
439 Zernitskaya, V. (2017). Vegetation of Eurasia from the last glacial maximum to present:
440 Key biogeographic patterns. *Quaternary Science Reviews*, *157*, 80–97.
441 https://doi.org/10.1016/j.quascirev.2016.11.022

442 Bird, J. P., Martin, R., Re, H., Gilroy, J., Burfield, I. J., Garnett, S. T., … Butchart, S. H. M.
443 (2020). Generation lengths of the world's birds and their implications for extinction risk.
444 *Conservation Biology*, *34*(5), 1252–1261. https://doi.org/10.1111/cobi.13486

445 Buchanan, G. M., Bond, A. L., Pearce-Higgins, J. W., Hilton, G. M., Crockford, N. J., & Kamp,
446 J. (2018). The potential breeding range of Slender-billed Curlew *Numenius tenuirostris*
447 identified from stable-isotope analysis. *Bird Conservation International*, *28*(2), 228–237.
448 https://doi.org/10.1017/S0959270916000551

449 Bushnell, B. (2014). BBMap. Retrieved from https://sourceforge.net/projects/bbmap/

450 Butchart, S. H. M., Lowe, S., Martin, R. W., Symes, A., Westrip, J. R. S., & Wheatley, H.
451 (2018). Which bird species have gone extinct? A novel quantitative classification approach.
452 *Biological Conservation*, *227*, 9–18. https://doi.org/10.1016/j.biocon.2018.08.014

453 Cahill, A. E., Aiello-Lammens, M. E., Caitlin Fisher-Reid, M., Hua, X., Karanewsky, C. J., Ryu,
454 H. Y., … Wiens, J. J. (2013). How does climate change cause extinction? *Proceedings of*
455 *the Royal Society B: Biological Sciences*, *280*(1750), 20121890.
456 https://doi.org/10.1098/rspb.2012.1890

457 Ceballos, G., Davidson, A., List, R., Pacheco, J., Manzano-Fischer, P., Santos-Barrera, G., &
458 Cruzado, J. (2010). Rapid decline of a grassland system and its ecological and conservation
459 implications. *PLoS ONE*, *5*(1), e8562. https://doi.org/10.1371/journal.pone.0008562

460 Chan, Y. L., Lacey, E. A., Pearson, O. P., & Hadly, E. A. (2005). Ancient DNA reveals
461 Holocene loss of genetic diversity in a South American rodent. *Biology Letters*, *1*(4), 423–
462 426. https://doi.org/10.1098/rsbl.2005.0354

463 Chattopadhyay, B., Garg, K. M., Mendenhall, I. H., & Rheindt, F. E. (2019). Historic DNA
464 reveals Anthropocene threat to a tropical urban fruit bat. *Current Biology*, *29*, R1269–
465 R1300. https://doi.org/10.1016/j

466 Chen, S., Zhou, Y., Chen, Y., & Gu, J. (2018). Fastp: An ultra-fast all-in-one FASTQ
467 preprocessor. *Bioinformatics*, *34*(17), i884–i890.
468 https://doi.org/10.1093/bioinformatics/bty560

469 Cloutier, A., Sackton, T. B., Grayson, P., Clamp, M., Baker, A. J., & Edwards, S. V. (2019).
470 Whole-genome analyses resolve the phylogeny of flightless birds (Palaeognathae) in the
471 presence of an empirical anomaly zone. *Systematic Biology*, *68*(6), 937–955.
472 https://doi.org/10.1093/sysbio/syz019

473 Crowley, T. J., & North, G. R. (1988). Abrupt climate change and extinction events in earth
474 history. *Science*, *240*(4855), 996–1002. https://doi.org/10.1126/science.240.4855.996

475 Danecek, P., Auton, A., Abecasis, G., Albers, C. A., Banks, E., DePristo, M. A., … Durbin, R.
476 (2011). The variant call format and VCFtools. *Bioinformatics*, *27*(15), 2156–2158.
477 https://doi.org/10.1093/bioinformatics/btr330

478 Dansgaard, W., Johnsen, S. J., Clausen, H. B., Dahl-Jensen, D., Gundestrup, N. S., Hammer, C.
479 U., … Bond, G. (1993). Evidence for general instability of past climate from a 250-kyr ice-
480 core record. *Nature*, *364*(6434), 218–220. https://doi.org/10.1038/364218a0

481 Darriba, D., Taboada, G. L., Doallo, R., & Posada, D. (2012, August 30). JModelTest 2: More
482 models, new heuristics and parallel computing. *Nature Methods*. Nature Publishing Group.
483 https://doi.org/10.1038/nmeth.2109

484 dos Reis, M., & Yang, Z. (2019). Bayesian molecular clock dating using genome-scale datasets.
485 In *Methods in Molecular Biology* (Vol. 1910, pp. 309–330). Humana Press Inc.
486 https://doi.org/10.1007/978-1-4939-9074-0_10

487 Engelmoer, M., & Roselaar, C. S. (1998a). Eurasian curlew *Numenius arquata*. In M. Engelmoer
488 & C. S. Roselaar (Eds.), *Geographical variation in waders* (pp. 213–223). Dordrecht,
489 Netherlands: Springer Science+Business Media B.V. https://doi.org/10.1007/978-94-011-
490 5016-3

491 Engelmoer, M., & Roselaar, C. S. (1998b). Whimbrel *Numenius phaeopus*. In M. Engelmoer &
492 C. S. Roselaar (Eds.), *Geographical variation in waders* (pp. 199–212). Dordrecht,
493 Netherlands: Springer Science+Business Media B.V. https://doi.org/10.1007/978-94-011-
494 5016-3

495 Felsenstein, J. (2009). PHYLIP (PHYLogeny Inference Package). Retrieved from
496 https://evolution.genetics.washington.edu/phylip.html

497 Foll, M., & Gaggiotti, O. (2008). A genome-scan method to identify selected loci appropriate for
498 both dominant and codominant markers: a Bayesian perspective. *Genetics*, *180*(2), 977–
499 993. https://doi.org/10.1534/genetics.108.092221

500 Frankham, R. (2005). Genetics and extinction. *Biological Conservation*, *126*(2), 131–140.
501 https://doi.org/10.1016/j.biocon.2005.05.002

502 Helm, A., Oja, T., Saar, L., Takkis, K., Talve, T., & Pärtel, M. (2009). Human influence lowers
503 plant genetic diversity in communities with extinction debt. *Journal of Ecology*, *97*(6),
504 1329–1336. https://doi.org/10.1111/j.1365-2745.2009.01572.x

505 IUCN. (2020). The IUCN Red List of Threatened Species. Version 2020-3. Retrieved from
506 https://www.iucnredlist.org

507 Jetz, W., Thomas, G. H., Joy, J. B., Redding, D. W., Hartmann, K., & Mooers, A. O. (2014).
508 Global distribution and conservation of evolutionary distinctness in birds. *Current Biology*,
509 *24*(9), 919–930. https://doi.org/10.1016/j.cub.2014.03.011

510 Johnson, M. G., Gardner, E. M., Liu, Y., Medina, R., Goffinet, B., Shaw, A. J., … Wickett, N. J.
511 (2016). HybPiper: Extracting coding sequence and introns for phylogenetics from high-
512 throughput sequencing reads using target enrichment. *Applications in Plant Sciences*, *4*(7),
513 1600016. https://doi.org/10.3732/apps.1600016

514 Jónsson, H., Ginolhac, A., Schubert, M., Johnson, P. L. F., & Orlando, L. (2013).
515 mapDamage2.0: Fast approximate Bayesian estimates of ancient DNA damage parameters.
516 In *Bioinformatics* (Vol. 29, pp. 1682–1684). Oxford Academic.
517 https://doi.org/10.1093/bioinformatics/btt193

518 Junier, T., & Zdobnov, E. M. (2010). The Newick utilities: high-throughput phylogenetic tree
519 processing in the UNIX shell. *Bioinformatics*, *26*(13), 1669–1670.
520 https://doi.org/10.1093/bioinformatics/btq243

521 Katoh, K., & Standley, D. M. (2013). MAFFT multiple sequence alignment software version 7:
522 Improvements in performance and usability. *Molecular Biology and Evolution*, *30*(4), 772–
523 780. https://doi.org/10.1093/molbev/mst010

524 Kearse, M., Moir, R., Wilson, A., Stones-Havas, S., Cheung, M., Sturrock, S., … Drummond, A.
525 (2012). Geneious Basic: An integrated and extendable desktop software platform for the
526 organization and analysis of sequence data. *Bioinformatics*, *28*(12), 1647–1649.
527 https://doi.org/10.1093/bioinformatics/bts199

528 Kirwan, G., Porter, R., & Scott, D. (2015). Chronicle of an extinction? A review of slender-billed
529 curlew records in the Middle East. *British Birds*, *108*(11), 669–682.

530 Koch, P. L., & Barnosky, A. D. (2006). Late quaternary extinctions: State of the debate. *Annual*
531 *Review of Ecology, Evolution, and Systematics*, *37*(1), 215–250.
532 https://doi.org/10.1146/annurev.ecolsys.34.011802.132415

533 Küpper, C., Stocks, M., Risse, J. E., Dos Remedios, N., Farrell, L. L., McRae, S. B., … Burke,
534 T. (2015). A supergene determines highly divergent male reproductive morphs in the ruff.
535 *Nature Genetics*, *48*(1), 79–83. https://doi.org/10.1038/ng.3443

536 Kuussaari, M., Bommarco, R., Heikkinen, R. K., Helm, A., Krauss, J., Lindborg, R., … Steffan-
537 Dewenter, I. (2009). Extinction debt: a challenge for biodiversity conservation. *Trends in*
538 *Ecology and Evolution*, *24*(10), 564–571. https://doi.org/10.1016/j.tree.2009.04.011

539 Larsson, A. (2010). abioscript. Retrieved from http://www.ormbunkar.se/phylogeny/abioscripts/

540 Lavinia, P. D., Kerr, K. C. R., Tubaro, P. L., Hebert, P. D. N., & Lijtmaer, D. A. (2016).
541 Calibrating the molecular clock beyond cytochrome b: Assessing the evolutionary rate of
542 COI in birds. *Journal of Avian Biology*, *47*(1), 84–91. https://doi.org/10.1111/jav.00766

543 Lemoine, N., & Böhning-Gaese, K. (2003). Potential impact of global climate change on species

richness of long-distance migrants. *Conservation Biology*, *17*(2), 577–586. https://doi.org/10.1046/j.1523-1739.2003.01389.x

Li, C., Riethoven, J. J. M., & Naylor, G. J. P. (2012). EvolMarkers: A database for mining exon and intron markers for evolution, ecology and conservation studies. *Molecular Ecology Resources*, *12*(5), 967–971. https://doi.org/10.1111/j.1755-0998.2012.03167.x

Li, H. (2011). A statistical framework for SNP calling, mutation discovery, association mapping and population genetical parameter estimation from sequencing data. *Bioinformatics*, *27*(21), 2987–2993. https://doi.org/10.1093/bioinformatics/btr509

Li, H. (2013). Aligning sequence reads, clone sequences and assembly contigs with BWA-MEM. *ArXiv Preprint*.

Li, H., & Durbin, R. (2009). Fast and accurate short read alignment with Burrows-Wheeler transform. *Bioinformatics*, *25*(14), 1754–1760. https://doi.org/10.1093/bioinformatics/btp324

Li, H., Handsaker, B., Wysoker, A., Fennell, T., Ruan, J., Homer, N., … Durbin, R. (2009). The sequence alignment/map format and SAMtools. *Bioinformatics*, *25*(16), 2078–2079. https://doi.org/10.1093/bioinformatics/btp352

Liu, L., Yu, L., & Edwards, S. V. (2010). A maximum pseudo-likelihood approach for estimating species trees under the coalescent model. *BMC Evolutionary Biology*, *10*(1), 302. https://doi.org/10.1186/1471-2148-10-302

Liu, X., & Fu, Y. X. (2015). Exploring population size changes using SNP frequency spectra. *Nature Genetics*, *47*(5), 555–559. https://doi.org/10.1038/ng.3254

Marques, D. A., Lucek, K., Sousa, V. C., Excoffier, L., & Seehausen, O. (2019). Admixture between old lineages facilitated contemporary ecological speciation in Lake Constance stickleback. *Nature Communications*, *10*(1), 1–14. https://doi.org/10.1038/s41467-019-12182-w

McKenna, A., Hanna, M., Banks, E., Sivachenko, A., Cibulskis, K., Kernytsky, A., … DePristo, M. A. (2010). The genome analysis toolkit: A MapReduce framework for analyzing next-generation DNA sequencing data. *Genome Research*, *20*(9), 1297–1303. https://doi.org/10.1101/gr.107524.110

Mirarab, S. (2014). Multi-locus-bootstrapping. Retrieved February 25, 2021, from https://github.com/smirarab/multi-locus-bootstrapping

Morozov, V. V. (2000). Current status of the southern subspecies of the whimbrel *Numenius phaeopus alboaxillaris* (Lowe 1921) in Russia and Kazakstan. *Wader Study Group Bulletin*, *92*(August), 30–37. Retrieved from http://scholar.google.com/scholar?hl=en&btnG=Search&q=intitle:Current+status+of+the+southern+subspecies+of+the+Whimbrel+Numenius+phaeopus+alboaxillaris+(Lowe+1921)+in+Russia+and+Kazakstan#0

Nakahama, N., Uchida, K., Ushimaru, A., & Isagi, Y. (2018). Historical changes in grassland area determined the demography of semi-natural grassland butterflies in Japan. *Heredity*, *121*(2), 155–168. https://doi.org/10.1038/s41437-018-0057-2

National Center for Biotechnology Information (NCBI). (1988). Retrieved from https://www.ncbi.nlm.nih.gov/

Okonechnikov, K., Conesa, A., & García-Alcalde, F. (2016). Qualimap 2: Advanced multi-sample quality control for high-throughput sequencing data. *Bioinformatics*, *32*(2), 292–294. https://doi.org/10.1093/bioinformatics/btv566

Pearce-Higgins, J. W., Brown, D. J., Douglas, D. J. T., Alves, J. A., Bellio, M., Bocher, P., … Soloviev, S. A. (2017). A global threats overview for Numeniini populations: synthesising expert knowledge for a group of declining migratory birds. *Bird Conservation International*, *27*, 6–34. https://doi.org/10.1017/S0959270916000678

Pimm, S. L., Jenkins, C. N., Abell, R., Brooks, T. M., Gittleman, J. L., Joppa, L. N., … Sexton, J. O. (2014). The biodiversity of species and their rates of extinction, distribution, and protection. *Science*, *344*(6187). https://doi.org/10.1126/science.1246752

Price, M. N., Dehal, P. S., & Arkin, A. P. (2010). FastTree 2 - Approximately maximum-likelihood trees for large alignments. *PLoS ONE*, *5*(3), e9490. https://doi.org/10.1371/journal.pone.0009490

Purcell, S., Neale, B., Todd-Brown, K., Thomas, L., Ferreira, M. A. R., Bender, D., … Sham, P. C. (2007). PLINK: A tool set for whole-genome association and population-based linkage analyses. *American Journal of Human Genetics*, *81*(3), 559–575. https://doi.org/10.1086/519795

Quinlan, A. R., & Hall, I. M. (2010). BEDTools: A flexible suite of utilities for comparing genomic features. *Bioinformatics*, *26*(6), 841–842. https://doi.org/10.1093/bioinformatics/btq033

R Core Team. (2018). R: A language and environment for statistical computing. R Foundation for Statistical Computing, Vienna, Austria. Retrieved from http://www.r-project.org/

Rambaut, A. (2018). FigTree 1.4.4. Retrieved from https://github.com/rambaut/figtree

Reis, M. Dos, & Yang, Z. (2011). Approximate likelihood calculation on a phylogeny for Bayesian estimation of divergence times. *Molecular Biology and Evolution*, *28*(7), 2161–2172. https://doi.org/10.1093/molbev/msr045

Roberts, D. L., Elphick, C. S., & Reed, J. M. (2010). Identifying anomalous reports of putatively extinct species and why it matters: Contributed paper. *Conservation Biology*, *24*(1), 189–196. https://doi.org/10.1111/j.1523-1739.2009.01292.x

Roberts, D. L., & Jarić, I. (2016). Inferring extinction in North American and Hawaiian birds in the presence of sighting uncertainty. *PeerJ*, *2016*(9), e2426. https://doi.org/10.7717/peerj.2426

Sharko, F. S., Boulygina, E. S., Rastorguev, S. M., Tsygankova, S. V, Tomkovich, P. S., & Nedoluzhko, A. V. (2019). Phylogenetic position of the presumably extinct slender-billed curlew, *Numenius tenuirostris*. *Mitochondrial DNA Part A: DNA Mapping, Sequencing, and Analysis*, *30*(4), 626–631. https://doi.org/10.1080/24701394.2019.1597862

Slater, G. S. C., & Birney, E. (2005). Automated generation of heuristics for biological sequence

comparison. *BMC Bioinformatics*, *6*(1), 1–11. https://doi.org/10.1186/1471-2105-6-31

Smit, A., Hubley, R., & Green, P. (2015). RepeatMasker Open-4.0.6. Retrieved from http://www.repeatmasker.org/

Stamatakis, A. (2014). RAxML version 8: a tool for phylogenetic analysis and post-analysis of large phylogenies. *Bioinformatics*, *30*(9), 1312–1313. https://doi.org/10.1093/bioinformatics/btu033

Tan, H. Z., Ng, E. Y. X., Tang, Q., Allport, G. A., Jansen, J. J. F. J., Tomkovich, pavel S., & Rheindt, F. E. (2019). Population genomics of two congeneric Palaearctic shorebirds reveals differential impacts of Quaternary climate oscillations across habitats types. *Scientific Reports*, *9*(1), 18172. https://doi.org/10.1038/s41598-019-54715-9

Török, P., Ambarlı, D., Kamp, J., Wesche, K., & Dengler, J. (2016). Step(pe) up! Raising the profile of the Palaearctic natural grasslands. *Biodiversity and Conservation*, *25*(12), 2187–2195. https://doi.org/10.1007/s10531-016-1187-6

Turvey, S. T., & Crees, J. J. (2019). Extinction in the Anthropocene. *Current Biology*, *29*(19), R982–R986. https://doi.org/10.1016/j.cub.2019.07.040

Urban, M. C. (2015). Accelerating extinction risk from climate change. *Science*, *348*(6234), 571–573. https://doi.org/10.1126/science.aaa4984

Wang, X., Maher, K. H., Zhang, N., Que, P., Zheng, C., Liu, S., … Liu, Y. (2019). Demographic histories and genome-wide patterns of divergence in incipient species of shorebirds. *Frontiers in Genetics*, *10*, 919. https://doi.org/10.3389/fgene.2019.00919

Wesche, K., Ambarlı, D., Kamp, J., Török, P., Treiber, J., & Dengler, J. (2016). The Palaearctic steppe biome: a new synthesis. *Biodiversity and Conservation*, *25*(12), 2197–2231. https://doi.org/10.1007/s10531-016-1214-7

Wingett, S. W., & Andrews, S. (2018). FastQ Screen: A tool for multi-genome mapping and quality control. *F1000Research*, *7*, 1338. https://doi.org/10.12688/f1000research.15931.2

Xu, H., Luo, X., Qian, J., Pang, X., Song, J., Qian, G., … Chen, S. (2012). FastUniq: A fast de novo duplicates removal tool for paired short reads. *PLoS ONE*, *7*(12), e52249. https://doi.org/10.1371/journal.pone.0052249

Yang, Z. (2007). PAML 4: Phylogenetic analysis by maximum likelihood. *Molecular Biology and Evolution*, *24*(8), 1586–1591. https://doi.org/10.1093/molbev/msm088

Zheng, X., Levine, D., Shen, J., Gogarten, S. M., Laurie, C., & Weir, B. S. (2012). A high-performance computing toolset for relatedness and principal component analysis of SNP data. *Bioinformatics*, *28*(24), 3326–3328. https://doi.org/10.1093/bioinformatics/bts606

Zimov, S. A., Chuprynin, V. I., Oreshko, A. P., Chapin, F. S., Reynolds, J. F., & Chapin, M. C. (1995). Steppe-tundra transition: A herbivore-driven biome shift at the end of the Pleistocene. *American Naturalist*, *146*(4), 765–794. https://doi.org/10.1086/285824

A

B

*N. tahitiensis* (2)

*N. phaeopus* (22)

*N. hudsonicus* (5)

*N. minutus* (2)

*N. arquata* (14)

*N. tenuirostris* (5)

CR

*N. madagascariensis* (3)

EN

*N. americanus* (4)

*N. borealis* (4)

CR

whimbrel clade

curlew clade

99

26

5 4 3 2 1 0

Million years before present



C

Interglacial

LGM

Glacial

35,277

22,330

3,612

276

100,000

50,000

0

Effective population size

1,000

10,000

100,000

Years before present

North Eurasia

35% genera extinct

arrival

agricultural land increase

forests expand

tundra, steppes dominate

North America

72% genera extinct

arrival

taiga dominates, with coastal tundra

ice sheets retreat